



## Research Paper

# EDA modified PANI/SWNTs nanocomposite for determination of Ni(II) metal ions



Megha A. Deshmukh<sup>a,b</sup>, Harshada K. Patil<sup>a,b</sup>, Gajanan A. Bodkhe<sup>a,b</sup>, Mikito Yasuzawa<sup>c</sup>, Pankaj Koinkar<sup>d</sup>, Arunas Ramanavicius<sup>e,f</sup>, Sadhna Pandey<sup>g</sup>, Mahendra D. Shirsat<sup>a,b,\*</sup>

<sup>a</sup> Department of Physics, Dr. Babasaheb Ambedkar Marathwada University, Aurangabad, MS 431 004, India

<sup>b</sup> RUSA-Center for Advanced Sensor and Technology, Dr. Babasaheb Ambedkar Marathwada University, Aurangabad, MS 431 004, India

<sup>c</sup> Department of Applied Chemistry, Tokushima University, Tokushima 770-8506, Japan

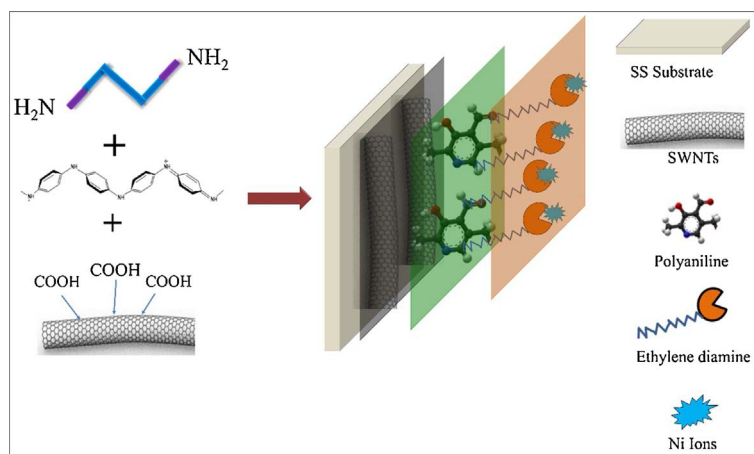
<sup>d</sup> Department of Optical Science, Tokushima University, Tokushima 770-8506, Japan

<sup>e</sup> Vilnius University, Faculty of Chemistry, Department of Physical Chemistry, Naugarduko St. 24, LT-03225 Vilnius, Lithuania

<sup>f</sup> State Research Institute Center for Physical Sciences and Technology, Laboratory of Bio Nano Technology, Savanoriu Ave. 231, LT-01108 Vilnius, Lithuania

<sup>g</sup> Department of Law, Dr. Babasaheb Ambedkar Marathwada University, Aurangabad, MS 431004, India

## GRAPHICAL ABSTRACT



Scheme 1 Representation of the formation of ethylenediamine modified PANI/SWNTs nanocomposite based electrochemical sensor for sensitive and selective detection of Ni(II) ions.

The formation of EDA modified PANI/SWNTs nanocomposite for detection of Ni(II) ions is shown in Scheme 1. The PANI/SWNTs nanocomposite structure was deposited on stainless steel (SS)-304 substrate through electrochemical route. Further the nanocomposite was modified with ethylenediamine via dip coating technique at room temperature.

## ARTICLE INFO

### Keywords:

Ethylenediamine  
DPV  
Nanocomposite sensor  
Electrochemical analysis  
Simultaneous detection

## ABSTRACT

Present communication deals with demonstration of a simple and facile approach towards electrochemical synthesis of single walled carbon nanotubes (SWNTs) and polyaniline (PANI) nanocomposite by electrochemical method and its application for the detection of Ni(II) metal ion from aqueous media in presence of ethylenediamine (EDA) chelating ligand. The modification of PANI/SWNTs nanocomposite with EDA was done through simple dip coating technique at room temperature. Polyaniline (PANI) and single walled carbon nanotubes (SWNTs) nanocomposite considered as a sensing backbone. EDA served the purpose of selective detection of Ni

\* Corresponding author at: RUSA-Center for Advanced Sensor Technology, Department of Physics, Dr. Babasaheb Ambedkar Marathwada University, Aurangabad, MS 431 004, India.  
E-mail address: [mdshirsat.phy@bamu.ac.in](mailto:mdshirsat.phy@bamu.ac.in) (M.D. Shirsat).

Nickel ion

(II) metal ion from aqueous media due to its ring-like structure. Ethylenediamine functionalized PANI/SWNTs nanocomposite (EDA-PANI/SWNTs) properties are evident from Electrochemical, Fourier transform infrared spectrometer (FTIR), Raman Spectroscopy, X-ray diffraction (XRD) and Atomic force microscope (AFM) analysis. Differential Pulse Voltammetry (DPV) technique was applied for the electrochemical analysis of Ni(II) ion. All recorded observations revealed that EDA modified PANI/SWNTs nanocomposite is suitable for the detection of Ni(II) ion.

## 1. Introduction

Contemporary carbon nanotubes (CNTs) and organic conducting polymer (OCP) based nanocomposite materials are grasping the attention of research communities due to their nanometer-sized structures and excellent properties [1–5]. High surface to volume ratio of nanocomposite materials is a key factor for the catalytic activities. The nanocomposite materials also show outstanding magnetic, optical, electronic, chemical, and electrochemical properties. In fact CNTs were first time discovered in 1991 by Sumio Iijima [6]. CNTs have excellent electrical properties as well as large surface area compared to other carbon based materials. CNTs shows improved mechanical properties like high tensile strength, flexibility due to its  $Sp^2$  bonded carbon structure [7,8]. CNTs are insoluble in water due to their polar nature [9] and likely advisable for the most of the analytical applications. CNTs can be functionalized covalently and non-covalently with a variety of materials to form the modified and composite electrode materials for plenty of applications with improved properties [10,11]. The extraordinary properties of CNTs, such as ease of functionalization ability, high surface to volume ratio, unique thermal, chemical, electrical and mechanical properties make them most preferred material for plenty of applications [12,13].

OCPs have enormous chemical, mechanical, optical and electrical properties and these properties as a result OCPs have been explored for various applications [14–17]. OCPs are enough flexible to make reversible changes in conductivity, color, mass and volume via doping, owing to their unique conjugated p-electron system [18–20]. Thus, OCPs viz., polyaniline (PANI), polypyrrole (PPy), and polythiophene (PTh) are having great deal of interest and widely applicable for electrode materials due to their high conductivity, high pseudo capacitance, low cost, environmental stability, and ease of synthesis [21–24]. However, in spite of all these suitable properties, OCPs have some limitations in their use due to the considerable volume change during the repeated intercalation and depletion of ions during charge and discharge process which is responsible for the largely decrease in mechanical stability of OCPs [25]. In this context, CNTs are promising materials to incorporate with OCPs to facilitate and improve the performance of OCPs for various applications due to their high surface area and high mechanical strength, electrical conductivity and chemical stability [26,27].

In 1994 Ajayan et al., has first reported the great advantage of the composite structure of CNTs-OCPs utilizing their individual countless profitable properties [28,29]. The combination of CNTs and OCPs based composite materials can achieve improved synergistic effect which means to achieve an efficient electro catalysis [30,31].

Thus, CNTs-OCPs composite structure have a wide range of applications in quite large number of fields such as, biomedical [32], orthopedic implants [33], treatment of periodontal diseases in dentistry [34], VOC sensors [35] etc.

In this regard, herein we have synthesized a single walled carbon nanotubes (SWNTs) – polyaniline (PANI) composite with ethylenediamine (EDA) as modifier chelating ligand for the detection of Ni(II) ion from the aqueous phase. PANI can interact with SWNTs via  $\pi$ - $\pi$  stacking which corresponds to non-covalent bonding. In the composite formation, SWNTs will act as a backbone of the structure surrounded by PANI molecules. EDA molecules will bind to the surface of PANI molecules and can firmly attach through  $\pi$ - $\pi$  interaction which gives the

ethylenediamine modified PANI-SWNTs nanocomposite for the selective and sensitive detection of Ni (II) ions.

## 2. Experimental

### 2.1. Materials and reagents

Aniline of reagent grade was purchased from Sigma Aldrich (Bangalore, India); Dodecyl benzene sulphonic acid sodium salt (DBSA) was procured from Kemphasol (Bombay, India) and it was used as surfactant and organic solvent to form fine suspension of SWNTs.  $H_2SO_4$  of HPLC grade acquired from Rankem (Bombay, India), SWNTs functionalized with carboxyl groups (-COOH) were purchased from Nanoshel LLC. Ethylenediamine (EDA) was procured from Fisher Scientific, 1-ethyl-3(3 (dimethyl amino) propyl)-Carbodiimide (EDC) was procured from Sigma Aldrich (Bangalore, India). Phosphate buffer with pH 7, and other chemicals were reagent grade quality and they were used as received. Stainless Steel (SS type 304, 0.5 mm thick and area  $1 \times 1 \text{ cm}^2$ ) purchased from MTI (Korea). Metal salt of  $Ni(NO_3)_2$  was procured from Fisher Scientific. All processes were performed in aqueous media and the preparation of the aqueous solutions were carried out using ultra-pure quality of water.

### 2.2. Synthesis of PANI/SWNTs nanocomposite

PANI/SWNTs nanocomposite was synthesized by an electrochemical method using cyclic voltammetry technique. Briefly, 0.25 M of aniline monomer and 0.5 M of  $H_2SO_4$  were added in distilled water (100 ml). It was 12% wt. of SWNTs in distilled water with respect to the concentration of aniline monomer. DBSA was added as a surfactant in the SWNTs + DI (Deionized water) solution to make fine suspension of the SWNTs with the ratio of 10:1 (DBSA:SWNTs) sonicated for 6 h. Resulting suspension of SWNTs was added slowly to the aniline +  $H_2SO_4$  solution, stirred for 20 min at room temperature using magnetic stirrer. The final electrolyte of aniline +  $H_2SO_4$  + SWNTs was utilized for the electrochemical synthesis of PANI/SWNTs nanocomposite.

Cyclic Voltammetry technique was used for electrochemical synthesis of PANI/SWNTs nanocomposite. SS substrate was used as a working electrode, Platinum plate as a counter electrode and Ag/AgCl as a reference electrode for synthesis of composite. The potential was scanned between 0.1–1.0 V for 20 cycles at the scan rate of 0.1 V/s. The composite formation on working electrode was observed by dark green colored coating with respect to the applied potential and cycles. The deposited dark green colored film was washed thoroughly with DI water to remove the excess monomer on a substrate surface and further dried at room temperature.

### 2.3. Preparation of EDA modified PANI/SWNTs nanocomposite

For the preparation of chelating ligand solution, 0.1 M of EDC (crosslinking agent) was added to the 0.01 M of EDA in 100 ml of distilled water and stirred for 20 min at room temperature. The electrochemically prepared PANI/SWNTs nanocomposite thin film was dipped in the EDA solution for 5 h at room temperature. After completion of dipping period the EDA modified nanocomposite film was rinsed through distilled water to remove the loosely bound EDA particles on

the surface and air dried.

#### 2.4. Preparation of Ni(II) ion solutions

For the analysis of metal ions from aqueous media, stock solutions of metal ion  $\text{Ni}(\text{NO}_3)_2$  was prepared.  $\text{Ni}(\text{NO}_3)_2$  metal ions were dispersed in the acetate buffer solutions of pH 2.1 to prepare an analyte solution and stirred for 20 min at room temperature to make a fine suspension of metal ions. The higher to lower concentration of metal ions were prepared by adding acetate buffer solution of respective pH for Ni(II) metal ion in the stock solution.

#### 2.5. Characterization methods

The electrochemical behavior of EDA modified nanocomposite before and after modification was studied by cyclic voltammetry technique, using a CHI 660C electrochemical workstation. Standard three electrode system, EDA-PANI/SWNTs deposited SS substrate as a working electrode, Platinum as a counter electrode and Ag/AgCl as a reference electrode was used for the evaluation. The potential was cycled between 0.1–1.0 V at the scan rate of 0.1 V/s. The electrochemical analysis of metal ions by EDA modified nanocomposite was carried out using differential pulse voltammetry technique (DPV) technique at room temperature, followed by a positive going DPV scan (with a step increment of 5 mV, amplitude of 50 mV, and pulse period of 0.2 s) in the potential range from  $-0.25$  to  $0.04$  for the analysis of Ni (II) ions.

The chemical composition of the nanocomposite before and after modification with EDA was evaluated by comparison of the Fourier transform infrared (FTIR) spectra of the modified and unmodified materials. FTIR analysis was performed with a Bruker-Alpha FTIR spectrometer equipped with an ATR. The FTIR spectra were collected over the range of  $600$ – $4000$   $\text{cm}^{-1}$ .

The fingerprint characteristics by which molecules can be identified such as study of vibrational, rotational and other low-frequency modes in a system were studied by Raman spectroscopy. Raman analysis was performed with a Seki technonics of make STR 150 Raman Spectrometer. The spectra of nanocomposite structure before and after modification with the EDA were collected over the range of  $100$ – $3000$   $\text{cm}^{-1}$ . X-Ray diffraction was performed with Bruker D8 Advance within the angle of  $5^\circ$ – $90^\circ$ .

Atomic force microscope (AFM) images were used for the morphological analysis of the synthesized nanocomposite. The AFM images of synthesized nanocomposite before and after EDA modification on SS substrate were analysed. A Park XE-7 atomic force microscope (AFM) was used for this investigation.

### 3. Results and discussion

#### 3.1. Electrochemical synthesis of PANI/SWNTs nanocomposite

The electrochemical deposition of PANI/SWNTs nanocomposite film was carried out on SS substrate through polymerization of aniline monomer with 12% wt. of SWNTs. Fig. 1 depicts the cyclic voltammogram recorded during growth of PANI/SWNTs nanocomposite with continuous potential scanning at 0.1 V/s in the potential range from 0.1 to 1.0 V. During electrochemical synthesis a thin dark green colored coating was observed on SS substrate, in a typical colour of PANI in the emeraldine salt form [36]. The positive potential scan articulates the oxidization of aniline exhibiting an anodic peaks A and B respectively. The thickness of the layer of nanocomposite was controlled by number of cycles applied. The peak height of voltammogram increased with increasing the number of potential cycles revealing that the synthesized nanocomposite is conducting in nature and regular growth of nanocomposite layer on the substrate.

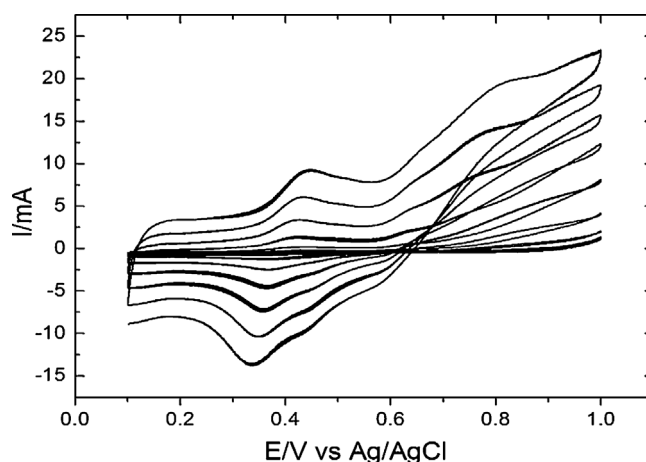


Fig. 1. Cyclic voltammogram recorded during the synthesis of PANI/SWNTs nanocomposite.

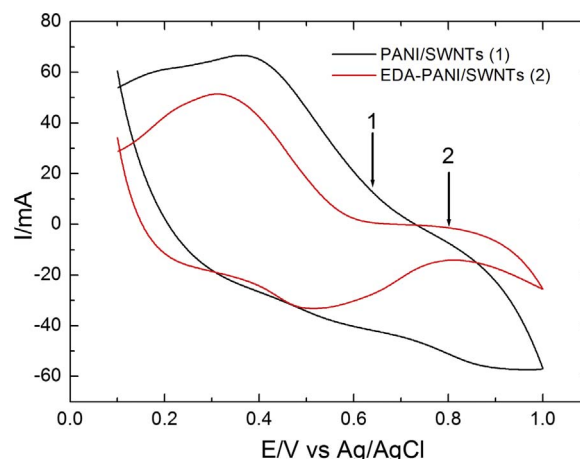


Fig. 2. Cyclic voltammograms of (a) PANI/SWNTs (Line 1) and (b) EDA-PANI/SWNTs (Line 2) nanocomposite structure in 0.5 M  $\text{H}_2\text{SO}_4$  at 0.1 V/s. (For interpretation of the references to colour in this figure legend, the reader is referred to the web version of this article.)

#### 3.2. Electrochemical analysis of PANI/SWNTs and EDA modified PANI/SWNTs nanocomposite

The electrochemical characterization of bare PANI/SWNTs nanocomposite and after modification with EDA molecules was confirmed by using electrochemical cyclic voltammetry technique (Fig. 2). The first anodic peak reveals the transition of aniline from leucoemeraldine to the most conducting protonated form of emeraldine of polyaniline. The second oxidizing peak of voltammogram confirms the oxidized form of polyaniline, relating to transformation of emeraldine to pernigraniline. This information reveals that both the voltammogram before and after modification are conducting in nature. Furthermore, from both the cyclic voltammograms of PANI/SWNTs and EDA-PANI/SWNTs it can be observed that unmodified PANI/SWNTs electrode showed increased current density and large area occupied in the voltammogram as compared to EDA-PANI/SWNTs electrode. This confirms the suppression of PANI/SWNTs nanocomposite by EDA and its domination in electrostatic interactions.

#### 3.3. Fourier transformation infrared (FTIR) spectroscopic analysis of PANI/SWNTs and EDA modified PANI/SWNTs nanocomposite

The FTIR spectra of PANI/SWNTs nanocomposite and EDA modified nanocomposite are shown in Fig. 3. The complexing mechanism of

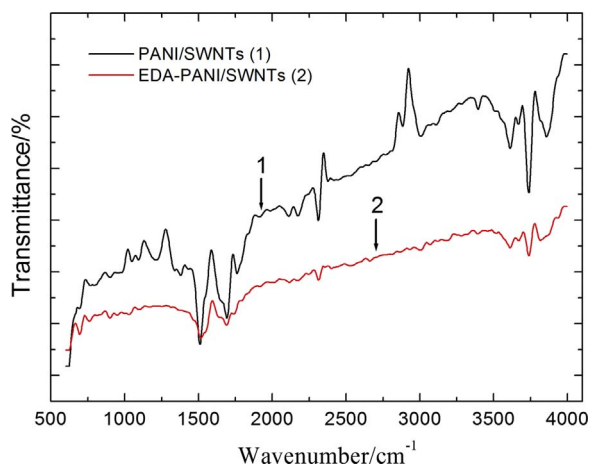


Fig. 3. FTIR spectra of PANI/SWNTs (Line 1) and EDA-PANI/SWNTs (Line 2) nanocomposite.

aniline monomer and SWNTs as well as modification of nanocomposite by EDA revealed from FTIR analysis. The PANI/SWNTs spectrum shows the basic bands for appearance of PANI molecules such as band at  $1433\text{ cm}^{-1}$  and  $1510\text{ cm}^{-1}$  for the benzoid and quinoid band formation which are the characteristic bands of the PANI. The band near about  $1220\text{ cm}^{-1}$  reveals emeraldine form and confirms the conducting nature of PANI. A broad peak at  $3404\text{ cm}^{-1}$  is due to the N–H stretching vibration of the aromatic amine. The bands at  $1219\text{ cm}^{-1}$  and  $795\text{ cm}^{-1}$  can be assigned for the C–N stretching of the secondary aromatic amine and C–H aromatic out of-plane bending vibration, respectively. The band at  $1048\text{ cm}^{-1}$  attributed for the presence of CNTs. All these bands are getting suppressed in the EDA modified PANI/SWNTs composite structure. These results confirm that EDA molecules are getting accumulated on the PANI/SWNTs nanocomposite and dominating the characteristic bands of PANI/SWNTs nanocomposite. In EDA modified spectra the vibrational modes attributed for the free amine groups such as  $\text{NH}_2$  scissoring at  $1523\text{ cm}^{-1}$ , C–N stretching at  $1098\text{ cm}^{-1}$ ,  $1033\text{ cm}^{-1}$  and NH wagging at  $942\text{ cm}^{-1}$ . The band at  $1686\text{ cm}^{-1}$  assigned for EDA is the  $\text{NH}_2$  (Primary amine).

### 3.4. XRD analysis of PANI/SWNTs and EDA modified PANI/SWNTs nanocomposite

The structural analysis of PANI/SWNTs nanocomposite before and after modification with EDA was carried out using X-Ray Diffraction (XRD) pattern (BRUKER D8 Advance). Fig. 4 shows the diffraction

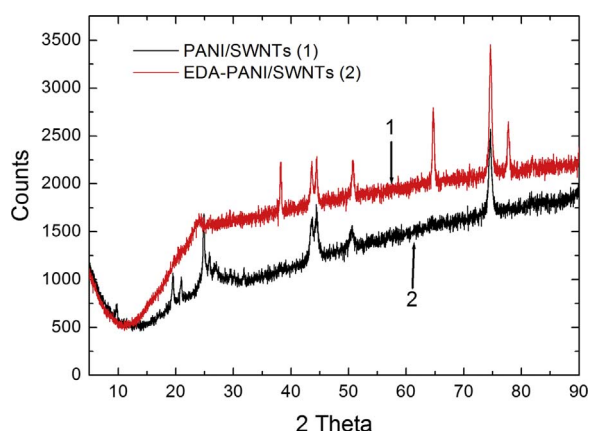


Fig. 4. XRD of (Black line) PANI/SWNTs and (Line 1) EDA modified PANI/SWNTs (Line 2) nanocomposite. (For interpretation of the references to colour in this figure legend, the reader is referred to the web version of this article.)

pattern of the nanocomposite before and after modification. The diffraction pattern for PANI/SWNTs and EDA-PANI/SWNTs nanocomposite was recorded broad scattering at  $2\theta$  values within  $10^\circ$ – $90^\circ$ . For PANI/SWNTs nanocomposite characteristic peaks for SWNTs appeared at  $2\theta = \sim 25^\circ$  and lower intensity peak at  $2\theta = \sim 43^\circ$ , as reported earlier [37]. For PANI typical peaks observed at  $2\theta = \sim 20^\circ$  corresponding to (020) crystal plane of PANI. The presence of peak at  $25^\circ$  accredited to the periodicity parallel to the polymer chain revealing the semi crystalline nature of material [38]. Thus, the observed characteristic peaks of PANI and SWNTs, indicating successful synthesis of PANI/SWNTs nanocomposite. In comparison of PANI/SWNTs nanocomposite and EDA modified nanocomposite, it has been observed that there is an increase in intensity of peaks after modification. After modification of PANI/SWNTs nanocomposite structure with EDA, the characteristic peaks observed in PANI/SWNTs nanocomposite structure seems to be suppressed due to accumulation of EDA molecules on nanocomposite structure. This result shows homogeneous coating of EDA onto the PANI/SWNTs nanocomposite surface indicating that PANI/SWNTs nanocomposite has successfully modified with EDA and is in well agreement with the results obtained from AFM.

### 3.5. Raman analysis of PANI/SWNTs and EDA modified PANI/SWNTs nanocomposite

Fig. 5 shows the Raman spectra of PANI/SWNTs and EDA modified PANI/SWNTs nanocomposite. In PANI/SWNTs nanocomposite, the presence of a broad G band at  $1592\text{ cm}^{-1}$  and D band at  $1351\text{ cm}^{-1}$  was observed. In the EDA modified nanocomposite, the D and G bands slightly shifted towards the left side due to the modification of nanocomposite structure. The presence of D induces the presence of amorphous disordered carbon structure of CNTs [39] and G band for the stretching band of C–C bond respectively [40]. The band at  $1309\text{ cm}^{-1}$  in the nanocomposite corresponds to the C–N<sup>+</sup> stretching, but in the EDA modified nanocomposite the same band is shifting to lower wavenumber at  $1198\text{ cm}^{-1}$  with less intensity. The shifting could be attributed to electrostatic interaction between the C–N<sup>+</sup> species of PANI and –COO species of SWNTs in nanocomposite [41]. But in EDA modified nanocomposite the intensity of same band is decreased, this might be due to dominating effect of EDA molecules over PANI/SWNTs electrostatic interaction. The enhancement of delocalization degree of C–N<sup>+</sup> segment shows increased intensity due to the presence of SWNTs [42] however, in modified nanocomposite intensity is decreases due to accumulation of EDA molecules on the nanocomposite. This clearly indicates that EDA ions got accumulated on the surface of nanocomposite.

### 3.6. Morphological analysis of PANI/SWNTs and EDA modified PANI/SWNTs nanocomposite

The AFM images for the PANI/SWNTs nanocomposite confirm rod like shape. The rod like structure formation of AFM reveals that SWNTs got coated by polyaniline. In this nanocomposite formation, CNTs are revealing as a backbone of the structure and polyaniline as the coating layer. The rod like shapes are clearly visible and separated from each other. In the structure of PANI/SWNTs nanocomposite, the presence of SWNTs is more evident. However in EDA modified PANI/SWNTs structure, SWNTs are hardly visible due to accumulation of EDA molecules on nanocomposite structure. In nanocomposite (PANI/SWNTs) longer and thicker structures appears compared to EDA modified PANI/SWNTs. From these observations it can be concluded that SWNTs got coated with PANI molecules and in modified nanocomposite whole composite structure is covered with EDA molecules. Fig. 6c shows histogram recorded from AFM scan images of PANI/SWNTs and EDA-PANI/SWNTs nanocomposite. Roughness of EDA modified PANI/SWNTs is more compared to unmodified nanocomposite. More roughness would be better to adsorb the analyte on surface area.

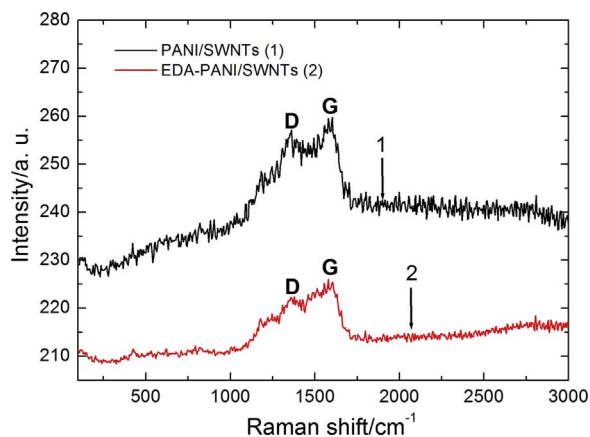


Fig. 5. Raman spectra of (Black line) PANI/SWNTs and (Red line) EDA modified PANI/SWNTs nanocomposite. (For interpretation of the references to colour in this figure legend, the reader is referred to the web version of this article.)

### 3.7. Differential pulse voltammetry of EDA modified PANI/SWNTs nanocomposite

EDA modified PANI/SWNTs nanocomposite electrode was immersed in to the measuring solution containing Ni(II) ions to adsorb the metal ion on to the surface of EDA-PANI/SWNTs electrode through complexation between the metal ions and EDA modified PANI/SWNTs electrode surface. The complexation of Ni(II) ions with EDA modified PANI/SWNTs was carried out in an acetate buffer solution of pH 2.1 containing different concentrations of Ni(II) ion by immersing the EDA-PANI/SWNTs electrode for 10 min with continuous stirring. The accumulation of Ni(II) ions on the EDA modified PANI/SWNTs electrode was carried out chemically without applying a reduction potential to avoid the contamination of working electrode as well as dislodging of electrode material. After accumulation of Ni(II) ions the electrode was taken off and washed with distilled water and transferred to a three electrode system containing blank solution of acetate buffer of pH 2.1 where EDA modified PANI/SWNTs utilized as working electrode, Pt plate as counter electrode and Ag/AgCl as reference electrode. Differential pulse voltammetry (DPV) for the EDA modified PANI/

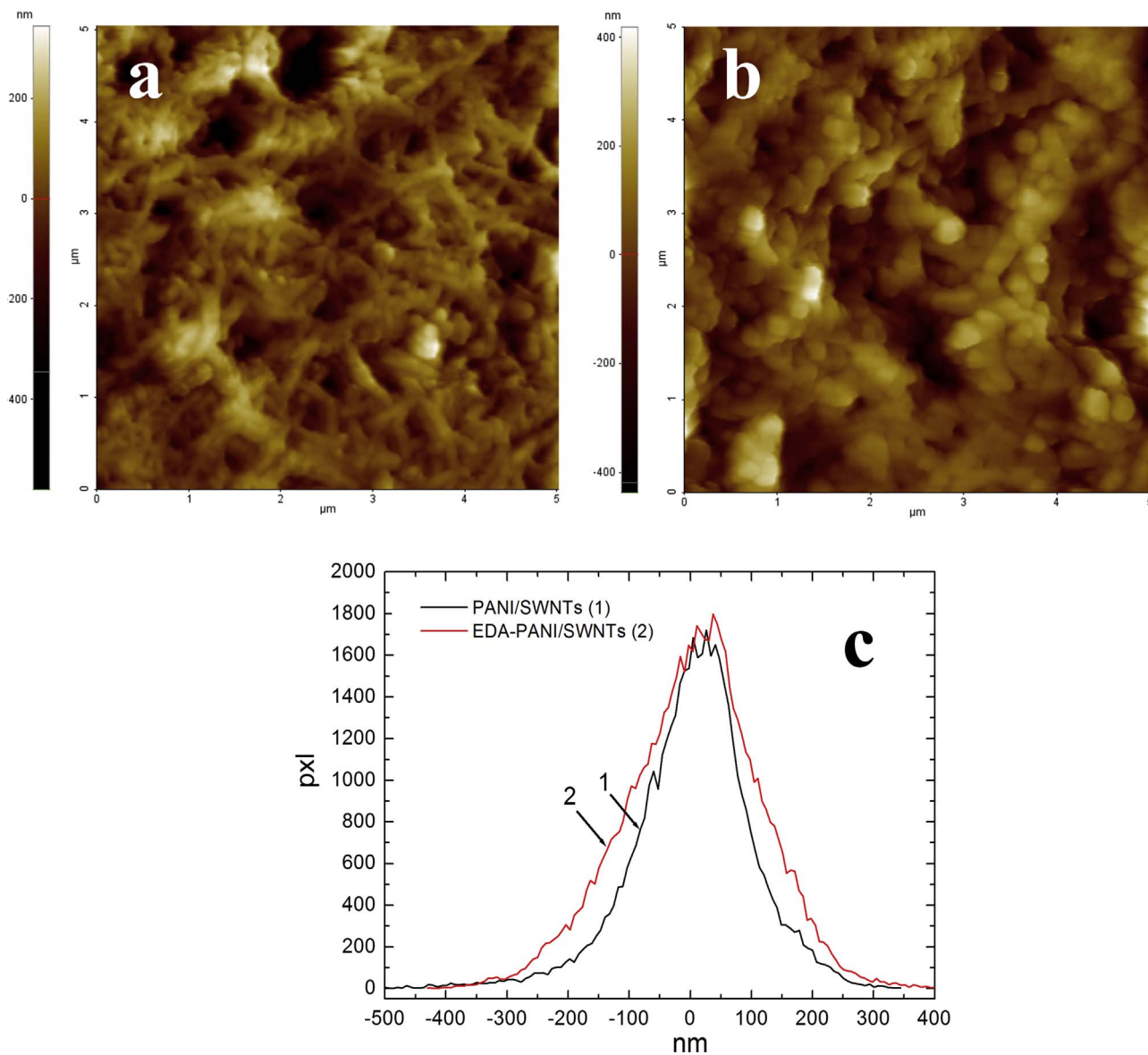


Fig. 6. AFM images of (a') PANI/SWNTs and (b) EDA modified PANI/SWNTs nanocomposite, (c) Histogram of PANI/SWNTs (Line 1) and EDA-PANI/SWNTs (Line 2). (For interpretation of the references to colour in this figure legend, the reader is referred to the web version of this article.)

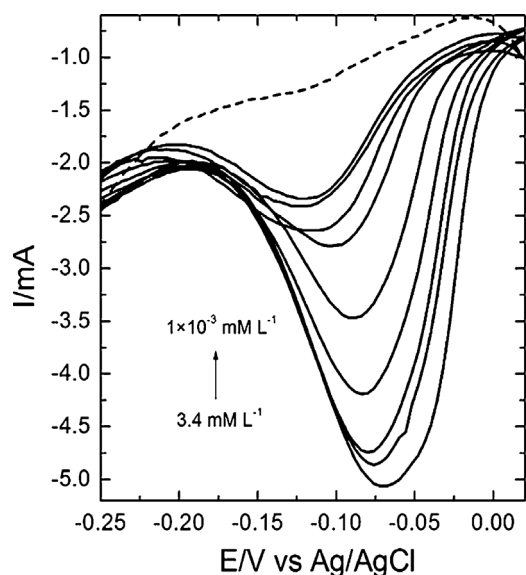


Fig. 7. Differential pulse voltammograms of SS electrodes modified by EDA modified PANI/SWNTs layer recorded in acetic acid buffer solution (pH 2.1), containing differential Ni(II) ion concentrations: 3.4 mM, 0.3 mM,  $6 \times 10^{-2}$  mM,  $3 \times 10^{-2}$  mM,  $6 \times 10^{-3}$  mM,  $3 \times 10^{-3}$  mM,  $2 \times 10^{-3}$  mM,  $1 \times 10^{-3}$  mM L<sup>-1</sup>, respectively.

SWNTs after this step recorded from  $-0.25$  to  $0.01$  V in a separate blank solution of  $0.5$  M H<sub>2</sub>SO<sub>4</sub>. DPV exhibit anodic peak in between  $0.0$  to  $-0.1$  V versus Ag/AgCl corresponding to the reduced of Ni(II) ions at EDA modified PANI/SWNTs surface. Overlapped differential pulse voltammogram curve shows response towards Ni(II) at EDA modified PANI/SWNTs layer modified SS-electrode for various concentrations (Fig. 7). However, no current peak was recorded after incubation of EDA modified PANI/SWNTs layer in blank solution (it is represented as reference curve (Dotted line)). The lower detection limit observed for Ni(II) ion is  $1 \times 10^{-3}$  mM L<sup>-1</sup>.

Very few reports are available on the DPV based electrochemical detection of Ni(II) ion. As listed in Table 1, spectroscopic and colorimetric techniques are widely used analytical techniques for accurate detection of metal ions. However, spectroscopic techniques are accountable for time consuming sample pre-treatment procedures and usage of sophisticated instrumentation [43]. In colorimetric techniques comparable colors from interfering substances can produce errors in results [44]. However, the reported ethylenediamine modified nanocomposite for detection of Ni(II) ion by electrochemical technique shows sensitive and selective response towards the Ni(II) ions.

Selectivity of the sensor is one of the most important characteristic of the any sensor. Ethylenediamine is a bidentate ligand that is able to form two coordinative bonds with a metal atom through the lone pair of

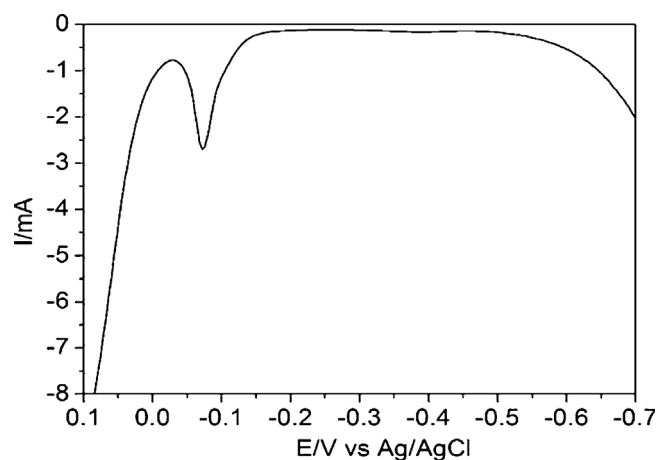


Fig. 8. DPV curve recorded in acetic acid buffer solution (pH 2.1) for selective detection of Ni(II) ions in the presence of Pb(II), Cd(II), Cu(II), Hg(II) and Co(II) ions.

electrons on both nitrogens [55]. Compared to alkaline earth and alkali metal cations the transition metal cations mostly shows strong affinity towards ethylenediamine [56]. In case of selective detection of Ni ions with ethylenediamine ligand, a single molecule of ethylenediamine is able to form two bonds to a transition metal ion, such as Ni(II). The bond formation can take place between the metal ion and the nitrogen atoms of ethylenediamine. The Ni(II) ion can form six such bonds; hence, a maximum of three ethylenediamine molecules can be attached to one Ni(II) ion [57]. However, EDA modified PANI/SWNTs nanocomposite shows selective response towards Ni(II) ion.

Fig. 8 shows DPV of Ni (II) ions in acetic acid buffer solution (pH 2.1) as the supporting electrolyte medium using EDA modified PANI/SWNTs. The EDA modified PANI/SWNTs electrode was immersed in a solution containing 2 of Pb(II), Cd(II), Hg(II), Co(II), Cu(II) ions for 10 min. The DPV plot shows the clear anodic peaks only for Ni(II). EDA showed selectivity towards only Ni(II) ions.

#### 4. Conclusions

Electrochemical synthesis and modification of PANI/SWNTs nanocomposite with EDA chelating ligand was successfully carried out. An electrochemical, spectroscopic and morphological characterization of PANI/SWNTs and EDA modified PANI/SWNTs confirms the information of chemical bonding and morphological differences between PANI/SWNTs nanocomposite and EDA modified PANI/SWNTs nanocomposite. The EDA modified PANI/SWNTs nanocomposite was used for detection of Ni(II) ion. The EDA modified PANI/SWNTs exhibit excellent sensing behaviour with lower detection limit of  $1 \times 10^{-3}$  mM L<sup>-1</sup>.

Table 1

Overview of some sensing materials used in electrochemical and optical sensors for the determination of Ni(II) ions.

Sr. No.	Sensing Material	Detection limit	Sensing technique	Ref.
01	A thio carboxylic acid derivative:2-aminocyclopent-1-ene-1-carbodithioic acid (ligand)	0.5 ppm	Colorimetric	[45]
02	Modified miswak fibers by NaOH (AT-Miswak-F).	2.1 ng mL <sup>-1</sup>	Infrared spectroscopy	[46]
03	Imine ligands, (E)-N1-(2-hydroxy-5 nitrobenzylidene) isonicotinoylhydrazine and 2-(4-fluoro benzylideneamino) benzenethiol	0.89 ng and 0.82 ng L <sup>-1</sup>	Spectrophotometric	[47]
04	Triangular silver nanoprisms (AgNPRs) stabilized with glutathione (GSH)	50 nM	Colorimetric	[48]
05	boron-doped diamond electrode	26.1 μM	Electrochemical	[49]
06	Hydrazone Derivative Immobilized on the Triacetyl Cellulose Membrane	$1.00 \times 10^{-10}$ mol L <sup>-1</sup>	Spectrophotometric	[50]
07	1 Leached Ag Nanoparticles	10 nM	Colorimetric	[51]
08	2 Quinoline	$5.0 \times 10^{-6}$ M	Colorimetric	[52]
09	3 Tetra(m-aminophenyl)porphyrin (Tm-APP)	3 ng L <sup>-1</sup>	Reversed-phase high-performance liquid chromatography (RP-HPLC)	[53]
10	Nafion-graphene dimethylglyoxime modified glassy carbon electrode	1.5 μg L <sup>-1</sup>	Adsorptive Stripping Voltammetry	[54]

## Acknowledgements

This work was supported by the Department of Science and Technology (DST)-SERB, New Delhi, India (Project No. SB/EMEQ-042/2013); Inter University Accelerator Center (IUAC), New Delhi, India (UFR No. 55305); Rashtriya Uchhatar Shiksha Abhiyan, Govt. of Maharashtra, India (RUSA/order/R & I/2016-17); UGC-SAP, New Delhi, India (F.530/16/DRS-I/2016(SAP-II)).

## References

- L. Ying-Ling, Effective approaches for the preparation of organo-modified multi-walled carbon nanotubes and the corresponding MWCNT/polymer nanocomposites, *Polym. J.* 48 (2016) 351–358.
- V. Catalina, P. Eugenia, L. Aitor, A. Marc, J. James, T. Alexandre, T. Ghazal, K. Adriona, R. Ilaria, S. Jose-Ramon, D. Eilfs, R. Leo, P. Abhay, J. Manus, Polyhydroxyalkanoate/carbon nanotube nanocomposites: flexible electrically conducting elastomers for neural applications, *Nanomedicine* 11 (2016) 2547–2563.
- C. Serena, P. Elisa, P. Andrea, R. Giacomo, Nanocomposites based on thermoplastic polymers and functional nanofiller for sensor applications, *Materials* 8 (2015) 3377–3427.
- P. Harshada, D. Megha, G. Sumedh, B. Gajanan, K. Asokan, Y. Mikito, K. Pankaj, S. Mahendra, Influence of oxygen ions irradiation on polyaniline/single walled carbon nanotubes nanocomposite, *Radiat. Phys. Chem.* 130 (2017) 47–51.
- D. Kunal, G. Prasanta, R. Arti, M. Ashok, S. Mahendra, Fe nanoparticles tailored poly(N-methyl pyrrole) nanowires matrix: a CHEMFET study in perspective of discrimination among electron donating analytes, *J. Phys. D: Appl. Phys.* 48 (2015) 1–8.
- S. Iijima, T. Ichihashi, Single-shell carbon nanotubes of 1-nm diameter, *Nature* 363 (1995) 603–605.
- J. Yang, X. Li, C. Liu, G. Ma, Changes of structure and electrical conductivity of multi-walled carbon nanotubes film caused by 3 MeV proton irradiation, *Appl. Surf. Sci.* 325 (2015) 235–241.
- P. Martins Jr., C. Alcântara, R. Resende, A. Ferreira, Carbon nanotubes directions and perspectives in oral regenerative medicine, *J. Dent. Res.* 92 (2013) 575–583.
- W. Chen, L. Duan, D. Zhu, Adsorption of polar and nonpolar organic chemicals to carbon nanotubes, *Environ. Sci. Technol.* 41 (2007) 8295–8300.
- S. Vashist, D. Zheng, K. Al-Rubeaan, J. Luong, F. Sheu, Advances in carbon nanotube based electrochemical sensors for bioanalytical applications, *Biotechnol. Adv.* 29 (2011) 169–188.
- P. Seligra, F. Nuevo, M. Lamanna, L. Famá, Covalent grafting of carbon nanotubes to PLA in order to improve compatibility, *Compos. Part B* 46 (2013) 61–68.
- Y. Luo, X. Wei, D. Cao, R. Bai, F. Xu, Y. Chen, Polystyrene-block-poly (tert-butyl methacrylate)/multiwall carbon nanotube ternary conducting polymer nanocomposites based on compatibilizers: preparation, characterization and vapor sensing applications, *Mater. Des.* 87 (2015) 149–156.
- A. Díez-Pascual, M. Naffakh, C. Marco, M. Gómez-Fatou, G. Ellis, Multiscale fiber-reinforced thermoplastic composites incorporating carbon nanotubes: a review, *Curr. Opin. Solid State Mater. Sci.* 18 (2014) 62–80.
- H. Park, T. Kim, J. Huh, M. Kang, J. Lee, H. Yoon, Anisotropic growth control of polyaniline nanostructures and their morphology-dependent electrochemical characteristics, *ACS Nano* 6 (2012) 7624–7633.
- M. Chang, T. Kim, H. Park, M. Kang, E. Reichmanis, H. Yoon, Imparting chemical stability in nanoparticulate silver via a conjugated polymer casing approach, *ACS Appl. Mater. Interfaces* 4 (2012) 4357–4365.
- Y. Zheng, W. Wang, G. Zhu, A. Wang, Enhanced selectivity for heavy metals using polyaniline-modified hydrogel, *Ind. Eng. Chem. Res.* 52 (2013) 4957–4961.
- O. Kwon, S. Park, H. Park, T. Kim, M. Kang, J. Jang, H. Yoon, Kinetically controlled formation of multidimensional poly(3,4-ethylenedioxythiophene) nanostructures in vapor-deposition polymerization, *Chem. Mater.* 24 (2012) 4088–4092.
- H. Yoon, Current trends in sensors based on conducting polymer nanomaterials, *Nanomaterials* 3 (2013) 524–549.
- S. Park, O. Kwon, J. Lee, J. Jang, H. Yoon, Conducting polymer-based nanohybrids transducers: a potential route to high sensitivity and selectivity sensors, *Sensors* 14 (2014) 3604–3630.
- H. Yoon, J. Jang, Conducting-polymer nanomaterials for high-performance sensor applications: issues and challenges, *Adv. Funct. Mater.* 19 (2009) 1567–1576.
- A. Burke, R & D considerations for the performance and application of electrochemical capacitors, *Electrochim. Acta* 53 (2007) 1083–1091.
- E. Frackowiak, V. Khomenko, K. Jurewicz, K. Lota, F. Béguin, Supercapacitors based on conducting polymers/nanotubes composites, *J. Power Sources* 153 (2006) 413–418.
- T. Girija, M. Sangaranarayanan, Analysis of polyaniline-based nickel electrodes for electrochemical supercapacitors, *J. Power Sources* 156 (2006) 705–711.
- J. Kim, K. Kim, K. Kim, Fabrication and electrochemical properties of carbon nanotube/polypyrrole composite film electrodes with controlled pore size, *J. Power Sources* 176 (2008) 396–402.
- C. Peng, S. Zhang, D. Jewell, G. Chen, Carbon nanotube and conducting polymer composites for supercapacitors, *Prog. Nat. Sci.* 18 (2008) 777–788.
- J. Issi, L. Langer, J. Heremans, C. Oik, Electronic properties of carbon nanotubes: experimental results, *Carbon* 33 (1995) 941–948.
- R. Ma, Study of electrochemical capacitors utilizing carbon nanotube electrodes, *J. Power Sources* 84 (1999) 126–129.
- M. Ates, Review study of (bio) sensor systems based on conducting polymers, *Mater. Sci. Eng. C* 33 (2013) 1853–1859.
- F. Al-Oqla, S. Sapuan, T. Anwer, M. Jawaid, M. Hoque, Natural fiber reinforced conductive polymer composites as functional materials: a review, *Synth. Met.* 206 (2015) 42–54.
- T. Lien, T. Lam, V. An, T. Hoang, D. Quang, D. Khieu, T. Tsukahara, Y. Lee, K. Kim, Multi-wall carbon nanotubes (MWCNTs)-doped polypyrrole DNA biosensor for label-free detection of genetically modified organisms by QCM and EIS, *Talanta* 80 (2010) 1164–1169.
- C. Peng, J. Jin, G. Chen, Comparative study on electrochemical co-deposition and capacitance of composite films of conducting polymers and carbon nanotubes, *Electrochim. Acta* 53 (2007) 525–537.
- D. Zhang, M. Kandadai, J. Cech, S. Roth, S. Currans, Poly(L-lactide) (PLLA)/multi-walled carbon nanotubes (MWCNT) composite: characterization and biocompatibility evaluation, *J. Phys. Chem. B* 110 (2006) 12910–12915.
- R. Spear, R. Cameron, Carbon nanotubes for orthopaedic implants, *Int. J. Mater. Form.* 1 (2008) 127–133.
- J. Yang, Z. Yao, C. Tang, B. Darvell, H. Zhang, L. Pan, J. Liu, Z. Chen, Growth of apatite on chitosan-multiwall carbon nanotube composite membranes, *Appl. Surf. Sci.* 255 (2009) 8551–8555.
- Y. Luo, X. Wei, D. Cao, R. Bai, F. Xu, Y. Chen, Polystyrene-block-poly (tert-butyl methacrylate)/multiwall carbon nanotube ternary conducting polymer nanocomposites based on compatibilizers: preparation, characterization and vapor sensing applications, *Mater. Des.* 87 (2015) 149–156.
- M.F. De Riccardis, M. Virginia, New method to obtain hybrid conducting nanocomposites based on polyaniline and carbon nanotubes, *Energia Ambiente e innovazione* 6 (2011) 86–95.
- O. Zhou, R. Fleming, D. Murphy, C. Chen, R. Haddon, A. Ramirez, S. Glarum, Defects in carbon nanostructures, *Science* 263 (1994) 1744–1747.
- A. Tursun, U. Aminam, R. Jamal, R. Adalet, Solid-state synthesis of polyaniline/single-walled carbon nanotubes: a comparative study with polyaniline/multi-walled carbon nanotubes, *Materials* 5 (2012) 1219–1231.
- M. Dresselhaus, G. Dresselhaus, R. Saito, A. Jorio, Raman spectroscopy of carbon nanotubes, *Phys. Rep.* 409 (2005) 47–99.
- M. Cochet, G. Louarn, S. Quillard, J. Buisson, S. Lefrant, Theoretical and experimental vibrational study of emeraldine in salt form. Part II, *J. Raman Spectrosc.* 31 (2000) 1041–1049.
- X. Yan, Z. Han, Y. Yang, B. Tay, Fabrication of carbon nanotube-polyaniline composites via electrostatic adsorption in aqueous colloids, *J. Phys. Chem. C* 111 (2007) 4125–4131.
- I. Šeděnková, M. Trchová, J. Stejskal, Thermal degradation of polyaniline films prepared in solutions of strong and weak acids and in water –FTIR and Raman spectroscopic studies, *Polym. Degrad. Stab.* 93 (2008) 2147–2157.
- Modi Wang, Ka-Ho Leung, Sheng Lin, Daniel Shiu-Hin Chan, Daniel W.J. Kwong, Chung-Hang Leung, Dik-Lung Ma, A colorimetric chemosensor for Cu<sup>2+</sup> ion detection based on an iridium(III) complex, *Sci. Rep.* 4 (2014) 1–7.
- A. Wallace Hayes, Principles and Methods of Toxicology, fifth edition, CRC Press, Taylor and Francis group, 2008.
- Y.L.N. Murthy, B. Govindh, B.S. Diwakar, K. Nagalakshmi, R. Singh, A simple inexpensive detection method of nickel in water using optical sensor, *Int. J. Chem. Technol. Res.* 3 (2011) 1285–1291.
- E.A. Moawed, M.A. Elghamry, M.A. Elagrasy, M.F. ElShahat, Determination of iron, cobalt and nickel ions from aqueous media using the alkali modified miswak, *J. Assoc. Arab Univ. Basic Appl. Sci.* 23 (2017) 43–51.
- B.N. Kumar, S. Kanchi, M.I. Sabela, K. Bisetty, N.V.V. Jyothi, Spectrophotometric determination of nickel (II) in waters and soils: novel chelating agents and their biological applications supported by DFT method, *Karbala Int. J. Mod. Sci.* 2 (2016) 239–250.
- N. Chen, Y. Zhang, H. Liu, H. Ruan, C. Dong, Z. Shen, A. Wu, A supersensitive probe for rapid colorimetric detection of nickel ion based on a sensing mechanism of anti-etching, *Sustain. Chem. Eng.* 4 (2016) 6509–6516.
- S. Neodo, M. Nie, J.A. Wharton, K.R. Stokes, Nickel-ion detection on a boron-doped diamond electrode in acidic media, *Electrochim. Acta* 88 (2013) 18–724.
- K. Alizadeh, N.A. Rad, A new optical sensor for selective monitoring of nickel ion based on a hydrazone derivative immobilized on the triacetyl cellulose membrane, *J. Anal. Bioanal. Technol.* 7 (2016) 1–6.
- W. Tianxiang, M. Zhanfang, Colorimetric detection of cobalt or nickel ions based on the change of the catalytic performance of leached Ag nanoparticles, *J. Nanosci. Nanotechnol.* 17 (2017) 4297–4303.
- X. Liu, Q. Lin, T. Wei, Y. Zhang, A highly selective colorimetric chemosensor for detection of nickel ions in aqueous solution, *New J. Chem.* 38 (2014) 1418–1423.
- Q. Hu, G. Yang, Y. Zhao, J. Yin, Determination of copper nickel, cobalt, silver, lead, cadmium, and mercury ions in water by solid-phase extraction and the RP-HPLC with UV–vis detection, *Anal. Bioanal. Chem.* 375 (2003) 831–835.
- K. Pokpas, N. Jahed, P.G. Baker, E.I. Iwuoha, Complexation-based detection of Nickel(II) at a graphene-chelate probe in the presence of cobalt and zinc by adsorptive stripping voltammetry, *Sensors* 17 (2017) 1711–1722.
- J.K. Beattle, conformational analysis of Tris(ethylenediamine) Complexes, *Acc. Chem. Res.* 4 (1971) 253–259.
- C. De Stefano, C. Foti, S. Sammartano, Interaction of polyamines with Mg<sup>2+</sup> and Ca<sup>2+</sup>, *J. Chem. Eng. Data* 44 (1999) 744–749.
- C. Watkins, G. Vige, Ethylenediamine complexes of copper (II) and nickel (II) in solutions of dimethyl sulfoxide, *J. Phys. Chem.* 80 (1976) 83–88.